

Synthesis, antitumor activity, and electrochemical behavior of some piperazinyl amidrazones

Raid Jamil Abdel-Jalil · Ehab Q. El Momani · Muawiah Hamad · Wolfgang Voelter ·
Mohammad S. Mubarak · Bianna H. Smith · Dennis G. Peters

Received: 28 March 2009 / Accepted: 15 December 2009 / Published online: 27 January 2010
© Springer-Verlag 2010

Abstract New piperazinyl amidrazones have been synthesized by direct interaction of the corresponding aryl hydrazones with the appropriate piperazine. On the basis of preliminary screening data for these new compounds, the antitumor activity of 1-(4-methylpiperazin-1-yl)-1,2-propanedione 1-[2-(4-chlorophenyl)hydrazone] and 1-(4-ethylpiperazin-1-yl)-1,2-propanedione 1-[2-(4-chlorophenyl)hydrazone] was evaluated. Mean 50% growth inhibition (GI_{50}), 50% cell killing (LC_{50}), and total growth inhibition (TGI) for both compounds were calculated on the basis of data obtained from 55 test cell lines. Mean GI_{50} is significantly lower for the methylpiperazine derivative (4.81 μM) compared with that of the ethylpiperazine derivative (4.92 μM) ($p > 0.01$); however, mean TGI is not measurably different ($p > 0.1$) for both

compounds (4.52 and 4.52 μM , respectively). Both compounds exhibit substantial antitumor activity against a number of cell lines at 4 μM concentration. It was found that the methylpiperazine derivative is more potent against leukemia cell lines (mean $GI_{50} = 4.73 \mu\text{M}$ and mean $TGI = 4.36 \mu\text{M}$), whereas the ethylpiperazine derivative is more potent against CNS cell lines ($GI_{50} = 4.68 \mu\text{M}$ and mean $TGI = 4.37 \mu\text{M}$). Cancers of the breast are least susceptible to methylpiperazine derivative activity compared with all other cell lines (mean $GI_{50} = 4.91 \mu\text{M}$). Melanomas and renal cancers are least susceptible to the ethylpiperazine derivative activity as compared with other cancer types (mean $GI_{50} = 5.06 \mu\text{M}$). Cyclic voltammetry has been employed to probe the electrochemical oxidation and reduction of the piperazinyl amidrazones at glassy carbon electrodes in dimethylformamide containing tetramethylammonium tetrafluoroborate.

R. J. Abdel-Jalil (✉)
Department of Chemistry, College of Science,
Sultan Qaboos University, Masqat, Oman
e-mail: jalil@squ.edu.jo; jalil@hu.edu.jo

E. Q. El Momani
Department of Chemistry, Faculty of Science,
Hashemite University, Zarqa, Jordan

M. Hamad
Department of Biological Sciences, Faculty of Science,
Hashemite University, Zarqa, Jordan

W. Voelter
Interfakultäres Institut für Biochemie der Universität Tübingen,
Hoppe-Seyler-Straße 4, Tübingen 72076, Germany

M. S. Mubarak
Department of Chemistry, University of Jordan, Amman, Jordan

B. H. Smith · D. G. Peters (✉)
Department of Chemistry, Indiana University,
Bloomington, IN 47405, USA
e-mail: peters@indiana.edu

Keywords Piperazinyl amidrazones · Cancer drugs ·
CNS cancers · Cyclic voltammetry

Introduction

One cannot overlook the significance of synthesizing and testing new compounds for potential therapeutic purposes, especially given the fact that the majority of drugs in use today came as a direct outcome of this endeavor [1]. Undoubtedly, cancer ranks high among human diseases still in dire need of effective therapy [2]. Notwithstanding the fact that the mechanisms of transformation, tumor genesis, and metastasis are much better understood now, advances in the area of anticancer therapy are occurring at a much slower pace [3]. Lack of a wide array of anticancer drugs able to capitalize on new discoveries regarding tumor genesis, coupled with the unique growth patterns of the

diverse repertoires of cancer, makes all approaches including the shotgun ones the more acceptable.

Due to their structural and therapeutic diversity, along with their commercial availability, piperazine derivatives have drawn considerable attention from organic and medicinal chemists. Piperazine molecular templates have been associated with a broad spectrum of biological activity; piperazine-based compounds have been employed as antibacterial [4], antidepressant [5], and antitumor [6] drugs, and as α -adrenoceptor antagonists [7], CCR5 receptor antagonists [8], 5-HT₇ receptor antagonists [9], and adenosine A_{2a} receptor antagonists [10]. Several piperazine derivatives have reached the stage of clinical application; a pyrimidinyl piperazinyl compound (buspirone, BuSpar[®]) is used to treat anxiety [11], and a 3-chlorophenyl piperazinyl drug (trazodone, Desyrel[®]) is an antidepressant [12].

Moreover, and equally pertinent to the present investigation, aryl amidrazones [possessing the $-\text{C}_6\text{H}_4-\text{NH}-\text{C}(\text{COCH}_3)=\text{N}-\text{NH}-\text{C}_6\text{H}_4-$ core] have recently been found to be potent corticotrophin-releasing factor (CRF) receptor antagonists [13]. Several publications have dealt with the synthesis and evaluation of thrombin inhibitors that incorporate an amidrazone functionality as a structural motif [14–16], and there is a report pertaining to the inactivation of lipoxygenase-1 from soybeans by open-chain and cyclic amidrazones [17].

With the preceding information in mind, we have synthesized a set of new piperazinyl amidrazones in a search for possible therapeutic agents. In this report we describe the chemical preparation and spectroscopic characterization of these compounds, the evaluation of their antitumor activity, and their electrochemical behavior at a vitreous carbon electrode in dimethylformamide containing tetramethylammonium tetrafluoroborate (TMABF₄). Although the electrochemistry of hydrazones has been examined in substantial detail [18–25], we are not aware of any previous study of the electrochemical oxidation and reduction of piperazinyl amidrazones.

Results and discussion

Chemistry

Syntheses of piperazinyl amidrazones **3–5** were carried out via the route shown in Scheme 1. Hydrazonyl chlorides were prepared according to a procedure described by Hussein and co-workers [26], which entails diazotization of an appropriate *p*-substituted aniline (**1a–1c**) followed by coupling with 3-chloro-2,4-pentanedione to afford **2a–2c**. Treatment of the hydrazonyl chloride with a *N*-substituted piperazine in the presence of triethylamine gives the desired piperazinyl amidrazone in good yield.

Different stoichiometric amounts of the piperazine (ranging from 1 to 5 equivalents) were used; the highest yields were obtained when a slight excess (1.25 equivalent) of the piperazine was employed. In the ¹H NMR spectra of the amidrazones, exchangeable protons give signals at 9.0–9.2 ppm, the α -methyl carbonyl protons resonate at 2.3–2.5 ppm, and the piperazinyl protons are revealed by two broad singlets at 2.5–3.5 ppm.

Biology

Evaluation of antitumor activity on a 55-human tumor cell line panel was conducted by the Developmental Therapeutics Program (DTP) of the National Cancer Institute (NCI), National Institutes of Health (NIH), Maryland, USA (<http://dtps7.ncicrf.gov>).

Preliminary screening of piperazinyl amidrazones

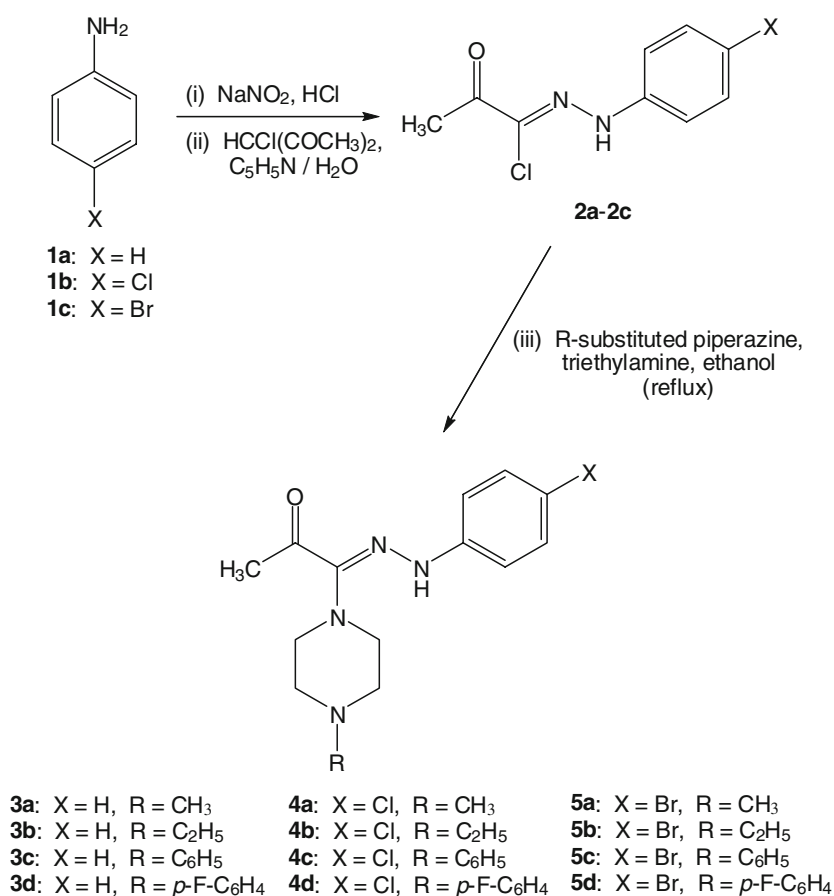
Preliminary screening data for the 12 different piperazinyl amidrazones prepared according to the protocol shown in Scheme 1 revealed that only two compounds, 1-(4-methylpiperazin-1-yl)-1,2-propanedione, 1-[2-(4-chlorophenyl)hydrazone] (**4a**) and 1-(4-ethylpiperazin-1-yl)-1,2-propanedione, 1-[2-(4-chlorophenyl)hydrazone] (**4b**), yielded percent test cell growth compared with untreated control cells (*PTC*) values of <32%, indicative of their reduced mitogenic and/or increased antigrowth potential.

Respective *PTC* values for the NCI-H460 (lung), MCF-7 (breast), and SF-268 (CNS) cell lines were found to be 9, 7, and 53% for **4a** and 6, 5, and 17% for **4b**. Therefore, both compounds were deemed suitable for additional assessment of antitumor activity. All other compounds (**3a–3d**, **4c**, **4d**, and **5a–5d**) exhibited *PTC* values of >32%, resulting in their exclusion from further testing.

Screening of **4a** and **4b**

Mean 50% growth inhibition (*GI*₅₀), 50% cell killing (*LC*₅₀), and total growth inhibition (*TGI*) values for **4a** and **4b** were calculated on the basis of data obtained from cultures on 55 and 54 cell lines, respectively (Table 1). Mean *GI*₅₀ was significantly lower for **4a** (4.81 μM) compared with that of **4b** (4.92 μM) (*t* test = 2.183; $0.05 > p > 0.01$). Mean *LC*₅₀ values for both compounds (4.17 and 4.19 μM , respectively) were statistically similar (*t* test = 0.84; $p < 0.5$). Additionally, the mean *TGI* for **4a** (4.47 μM) was not significantly different (*t* test = 1.418; $p > 0.1$) from that of **4b** (4.52 μM). It is worth noting that the range of activity for both compounds was narrow for all three parameters (Table 1). Furthermore, both compounds exhibited significant antitumor activity against a number of cell lines at 4 μM concentration.

Scheme 1

**Table 1** Mean antitumor activity of **4a** and **4b** as tested on 55 and 54 different cell lines, respectively

Dose response parameter	Compound	
	4a (μM)	4b (μM)
<i>GI</i> ₅₀ (mean ± standard deviation)	4.81 ± 0.181	4.92 ± 0.326
<i>GI</i> ₅₀ (range)	4.49–5.50	4.00–5.72
<i>LC</i> ₅₀ (mean ± standard deviation)	4.17 ± 0.097	4.19 ± 0.147
<i>LC</i> ₅₀ (range)	4.00–4.42	4.00–4.80
<i>TGI</i> (mean ± standard deviation)	4.47 ± 0.125	4.52 ± 0.229
<i>TGI</i> (range)	4.00–9.93	4.00–5.27

A detailed analysis of *GI*₅₀, *LC*₅₀, and *TGI* per cancer-type subpanel is provided in Table 2, and a number of interesting points are revealed. On the basis of the *GI*₅₀ parameter, **4a** was more potent against leukemia cell lines (mean *GI*₅₀ = 4.73 μM), non-small cell lung cancers (mean *GI*₅₀ = 4.76 μM), colon cancer (mean *GI*₅₀ = 4.76 μM), and CNS cancers (mean *GI*₅₀ = 4.77 μM). On the other hand, **4b** was more potent against CNS cell lines with a mean *GI*₅₀ of 4.68 μM. The least susceptible cell lines against **4a** activity were cancers of the breast, prostate, and ovaries; mean *GI*₅₀ concentrations were 4.91, 4.88, and 4.87 μM, respectively. Least susceptible cell lines against **4b** activity

were melanomas, renal cancers, and non-small lung cancers; mean *GI*₅₀ concentrations were 5.06, 5.06, and 4.97 μM, respectively.

On the basis of the *TGI* dose-response parameter, **4a** was more potent against leukemia cell lines (mean *TGI* = 4.36 μM) and non-small cell lung cancers (mean *TGI* = 4.19 μM), whereas **4b** was most potent against CNS cell lines with a mean *TGI* of 4.37 μM. The least susceptible cell lines against **4a** antitumor activity were cancers of the kidney, ovary, and breast, in addition to melanomas; mean *TGI* concentrations were 4.53, 4.53, 4.52, and 4.52 μM, respectively. Least susceptible cell lines against **4b** antitumor activity were melanomas, renal cancer, and non-small cell lung cancers; mean *TGI* concentrations were 4.64, 4.62, and 4.57 μM, respectively.

Once again, the range for antitumor activity considering all three dose-response parameters was narrow. Both compounds exhibited antitumor activity against some tumor cell lines at 4.0 μM concentration. Most notable was the activity of **4b** against the breast cancer MCF7 cell line where 4.0 μM was the concentration of *GI*₅₀, *LC*₅₀, and *TGI*.

From the results of this study, it is clear that both **4a** and **4b** bear significant antitumor activity against a number of human tumor cell lines, especially leukemia, non-small cell lung cancer, and CNS cancers. Given the finding that the

Table 2 Mean antitumor activity of **4a** and **4b** against various tumor-cell-line subpanels as defined by type of cancer

Cell-line subpanel (no. of cell lines)	Compound 4a		
	Mean GI_{50} (range) (μ M)	Mean LC_{50} (range) (μ M)	Mean TGI (range) (μ M)
Leukemia (5)	4.73 \pm 0.77 (4.62–4.82)	4.07 \pm 0.076 (4.00–4.18)	4.36 \pm 0.134 (4.14–4.50)
Non-small cell lung cancer (9)	4.76 \pm 0.115 (4.49–4.93)	4.13 \pm 0.091 (4.00–4.25)	4.19 \pm 0.166 (4.00–4.57)
Colon cancer (7)	4.76 \pm 0.045 (4.71–4.81)	4.16 \pm 0.099 (4.00–4.27)	4.46 \pm 0.072 (4.34–4.54)
CNS cancer (5)	4.77 \pm 0.079 (4.69–4.86)	4.15 \pm 0.089 (4.00–4.24)	4.45 \pm 0.088 (4.33–4.55)
Melanoma (7)	4.80 \pm 0.193 (4.68–4.88)	4.21 \pm 0.065 (4.11–4.27)	4.51 \pm 0.070 (4.40–4.57)
Ovarian cancer (5)	4.87 \pm 0.051 (4.73–5.29)	4.23 \pm 0.059 (4.19–4.32)	4.53 \pm 0.104 (4.47–4.71)
Renal cancer (8)	4.84 \pm 0.082 (4.74–4.99)	4.22 \pm 0.044 (4.16–4.30)	4.53 \pm 0.057 (4.48–4.64)
Prostate cancer (2)	4.88 \pm 0.021 (4.75–4.85)	4.07 \pm 0.099 (4.00–4.14)	4.42 \pm 0.099 (4.35–4.49)
Breast cancer (7)	4.91 \pm 0.452 (4.75–5.50)	4.16 \pm 0.148 (4.00–4.42)	4.52 \pm 0.185 (4.36–4.93)
Cell-line subpanel (no. of cell lines)	Compound 4b		
	Mean GI_{50} (range) (μ M)	Mean LC_{50} (range) (μ M)	Mean TGI (range) (μ M)
Leukemia (5)	4.93 \pm 0.085 (4.84–5.04)	4.17 \pm 0.056 (4.09–4.21)	4.55 \pm 0.049 (4.49–4.60)
Non-small cell lung cancer (9)	4.97 \pm 0.467 (4.21–5.72)	4.21 \pm 0.163 (4.00–4.59)	4.57 \pm 0.320 (4.00–5.22)
Colon cancer (7)	4.88 \pm 0.157 (4.71–5.13)	4.15 \pm 0.137 (4.00–4.30)	4.45 \pm 0.234 (4.00–4.66)
CNS cancer (5)	4.68 \pm 0.168 (4.39–4.82)	4.14 \pm 0.100 (4.00–4.27)	4.37 \pm 0.215 (4.00–4.55)
Melanoma (7)	5.06 \pm 0.288 (4.74–5.63)	4.23 \pm 0.254 (4.00–4.80)	4.64 \pm 0.308 (4.34–5.27)
Ovarian cancer (5)	4.93 \pm 0.301 (4.74–5.33)	4.15 \pm 0.085 (4.00–4.21)	4.48 \pm 0.075 (4.33–4.60)
Renal cancer (8)	5.06 \pm 0.280 (4.84–5.38)	4.27 \pm 0.044 (4.18–4.33)	4.62 \pm 0.080 (4.51–4.76)
Prostate cancer (2)	4.88 \pm 0.156 (4.77–4.99)	4.22 \pm 0.014 (4.21–4.23)	4.55 \pm 0.085 (4.49–4.61)
Breast cancer (7)	4.85 \pm 0.517 (4.00–5.61)	4.11 \pm 0.160 (4.00–4.44)	4.43 \pm 0.263 (4.00–4.90)

range of antitumor activity of both agents against the various tumor cell lines was very narrow, it can be stated that both compounds possess generalized antitumor activity.

Yet to be elucidated is the exact mechanism by which either compound suppresses cancer growth. This issue is under intensive study, and results will be published in due course.

Cyclic voltammetric behavior of piperazinyl amidrazones

Cyclic voltammograms were acquired for the reduction and oxidation of each of the piperazinyl amidrazones at a glassy carbon electrode in DMF containing 0.050 M TMABF₄. Table 3 provides a compilation of the cathodic and anodic peak potentials for these compounds. A representative cyclic voltammogram recorded at a scan rate of 100 mV s⁻¹ for a 2.0 mM solution of **4a** in DMF-0.050 M TMABF₄ is shown in Fig. 1. Four cathodic peaks are observed with peak potentials of -1.89, -2.56, -2.75, and -2.91 V versus SCE, and a single oxidation peak appears at -0.35 V versus SCE. Note that the third cathodic peak is a shoulder on the side of the fourth peak. It is significant

that the main anodic peak is seen only after a preceding negative-going scan. Moreover, associated with the main anodic peak is another small anodic peak at +0.06 V as well as a small cathodic peak at -0.60 V. In general, those compounds (**3a–3d**) without an aryl chlorine or bromine substituent exhibit three main cathodic peaks and one main anodic peak, whereas the halogenated species (**4a–4d** and **5a–5d**) show four main cathodic peaks (the last of which is not always well defined) along with one main anodic peak.

To aid further interpretation of the cyclic voltammograms for the piperazinyl amidrazones, we carried out separate cyclic voltammetry studies of the oxidation and reduction of 2.0 mM solutions of 1,4-dimethylpiperazine (**6**), 4-chloro-*N*-methylaniline (**7**), and pyruvaldehyde 1-phenylhydrazone (1-(2-phenylhydrazono)propan-2-one, **8**) at a glassy carbon electrode in DMF containing 0.050 M TMABF₄. No electroactivity for **6** was observed within the range of potentials from +0.26 to -3.05 V versus SCE, which reveals that a tertiary amine (*N*-alkylated piperazine) undergoes neither oxidation nor reduction under the conditions of our experiments. When the electrochemistry of **7** was examined, only a single cathodic peak was observed at -2.85 V versus SCE, which can be attributed to two-electron reductive cleavage

Table 3 Cathodic and anodic peak potentials for piperaziny amidrazones

Compound	Cathodic peak potentials (V vs. SCE)			Anodic peak potential (V vs. SCE)	
3a	-1.95	-2.62	-2.78	-0.43	
3b	-1.94	-2.58	-2.77	-0.44	
3c	-1.93	-2.58	-2.76	-0.40	
3d	-1.92	-2.57	-2.73	-0.39	
4a	-1.89	-2.56	-2.75	-2.91	-0.35
4b	-1.88	-2.55	-2.74	-2.88	-0.36
4c	-1.86	-2.51	-2.73	-2.89	-0.33
4d	-1.86	-2.49	-2.73	-2.86	-0.33
5a	-1.90	-2.40	-2.59	-2.81	-0.36
5b	-1.89	-2.39	-2.60	-2.78	-0.34
5c	-1.88	-2.38	-2.54	-2.75	-0.32
5d	-1.89	-2.37	-2.57	-2.78	-0.32

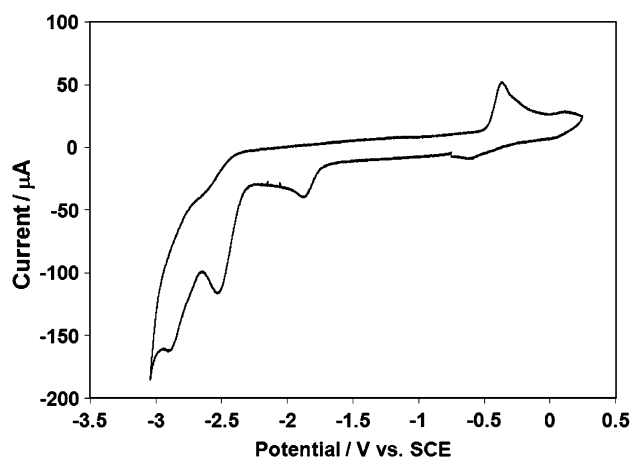


Fig. 1 Cyclic voltammogram recorded with a glassy carbon electrode (area = 0.071 cm²) at a scan rate of 100 mV s⁻¹ for a 2.0 mM solution of 1-(4-methylpiperazin-1-yl)-1,2-propanedione, 1-[2-(4-chlorophenyl)hydrazone] (**4a**) in DMF containing 0.050 M TMBF₄. Potential was scanned from -0.76 to -3.05 to +0.26 to -0.76 V versus SCE

of the aryl carbon–chlorine bond; thus, we believe that the fourth cathodic peak listed in Table 3 for compounds **4a–4d** arises from reduction of the aromatic carbon–chlorine bond. A cyclic voltammogram for **8** showed a well-resolved cathodic peak at -1.69 V versus SCE, two partially overlapping cathodic peaks at -2.38 and -2.46 V versus SCE, and an anodic peak at +0.04 V versus SCE. Thus, the electrochemical behavior of compounds **3a** and **8** is qualitatively similar, which leads us to conclude that the observed electroactivity of **3a** resides in its H₃C–CO–C=N–NH–C₆H₅ moiety; apparently, the presence of the methyl piperaziny substituent of **3a** shifts the cathodic and anodic peak potentials significantly toward more negative values in comparison with compound **8**.

A separate and more thorough investigation of the electrochemistry of these compounds is planned for the future, so that details of the redox reactions can be delineated, and intermediates and products arising from these electron-transfer processes can be identified.

Experimental

Instrumentation and chemicals

Melting points (°C) were measured with a SMP2 Stuart apparatus. All new compounds were analyzed for C, H, and N, and the observed results agreed with the calculated percentages to within ±0.4%. We obtained ¹H and ¹³C NMR spectra with a Bruker DPX-300 spectrometer; chemical shifts are reported in ppm relative to TMS as internal standard. Infrared (IR) spectra were recorded as KBr discs on a Nicolet-MAGNA-IR-560 spectrometer. Solid-probe high-resolution mass spectral data were acquired with the aid of a Thermo Electron Corporation MAT 95XP-Trap instrument, operated in the positive chemical-ionization (CI) mode with methane as the reagent gas.

We purchased and used as received from commercial sources 3-chloro-2,4-pentanedione and the *N*-substituted piperazines. Dimethylformamide (DMF, ACS spectrophotometric grade, 99.8%) was employed, without further purification, as the solvent for electrochemical experiments. Tetramethylammonium tetrafluoroborate (TMBF₄), used as the supporting electrolyte, was recrystallized from water-methanol and thoroughly dried by continuous storage in a vacuum oven at 80 °C. Deaeration of solutions for cyclic voltammetry was accomplished with zero-grade argon. To aid in the interpretation of cyclic voltammograms for the various piperaziny amidrazones, commercially available 1,4-dimethylpiperazine, 4-chloro-*N*-methylaniline,

and pyruvaldehyde 1-phenylhydrazone -1-(2-phenylhydrazono)propan-2-one were used as model compounds.

Synthesis of hydrazonyl chlorides **2a–2c**

These compounds were prepared via the Japp-Klingemann reaction involving coupling of arenediazonium salts to 3-chloro-2,4-pentanedione [26]. ¹H NMR and ¹³C NMR spectra were identical with those described in Ref. [26].

General procedure for the synthesis of piperazinyl amidrazones **3–5**

To a stirred solution of the appropriate hydrazonyl chloride **2** (0.10 mol) and triethylamine (0.11 mol) in 40 cm³ ethanol, the appropriate piperazine (0.125 mol) was added dropwise over 10 min at room temperature. Then the reaction mixture was refluxed for 3 h. Finally, the solvent was removed in vacuo, and the residue was purified by means of flash column chromatography with dichloromethane–ethyl acetate (4:1 v/v) to give the desired piperazinyl amidrazone.

1-(4-Methylpiperazin-1-yl)-1,2-propandione, 1-(2-phenylhydrazone) (3a, C₁₄H₂₀N₄O)

Yield 1.96 g (75%); m.p.: 79–80 °C; *R*_f = 0.63; ¹H NMR (CDCl₃): δ = 9.08 (s, 1H, NH), 6.91–7.30 (m, 5H, C₆H₅), 3.03, 2.46 (each bs, each 4H, piperazine), 2.36 (s, 3H, NCH₃), 2.30 (s, 3H, COCH₃); ¹³C NMR (CDCl₃): δ = 194.90 (C=O), 143.39 (C=N), 114.12, 122.08, 129.44, 142.59 (C₆H₅), 55.88, 47.79 (piperazine), 46.47 (CH₃), 25.71 (COCH₃); IR (KBr): $\bar{\nu}$ = 3,420, 1,678, 1,537 cm⁻¹; HRMS (CI): *m/z* = 261.1709 ([M + H]⁺, calcd for C₁₄H₂₁N₄O 261.1715) ppm.

1-(4-Ethylpiperazin-1-yl)-1,2-propandione, 1-(2-phenylhydrazone) (3b, C₁₅H₂₂N₄O)

Yield 2.15 g (78%); m.p.: 50–54 °C; *R*_f = 0.67; ¹H NMR (CDCl₃): δ = 9.10 (s, 1H, NH), 6.94–7.31 (m, 5H, C₆H₅), 3.06, 2.51 (each bs, each 4H, piperazine), 2.44 (q, *J* = 7.2 Hz, 2H, CH₂CH₃), 2.37 (s, 3H, COCH₃), 1.09 (t, *J* = 7.2 Hz, 3H, CH₂CH₃); ¹³C NMR (CDCl₃): δ = 194.94 (C=O), 143.47 (C=N), 114.11, 122.06, 129.45, 142.60 (C₆H₅), 53.64, 47.86 (piperazine), 52.61 (CH₂CH₃), 25.72 (COCH₃), 12.07 (NCH₂CH₃); IR (KBr): $\bar{\nu}$ = 3,420, 1,678, 1,537 cm⁻¹; HRMS (CI): *m/z* = 275.1862 ([M + H]⁺, calcd for C₁₅H₂₃N₄O 275.1872) ppm.

1-(4-Phenylpiperazin-1-yl)-1,2-propandione, 1-(2-phenylhydrazone) (3c, C₁₉H₂₂N₄O)

Yield 2.40 g (74%); m.p.: 158–162 °C; *R*_f = 0.42; ¹H NMR (CDCl₃): δ = 9.22 (s, 1H, NH), 6.90–7.37 (m, 10H, Ar), 3.26, 3.25 (each bs, each 4H, piperazine), 2.46 (s, 3H, COCH₃); ¹³C NMR (CDCl₃): δ = 195.10 (C=O), 151.50

(C=N), 114.22, 116.42, 120.14, 122.30, 129.24, 129.56, 142.53, 143.22 (Ar), 50.22, 48.12 (piperazine), 25.81 (COCH₃); IR (KBr): $\bar{\nu}$ = 3,420, 1,678, 1,537 cm⁻¹; HRMS (CI): *m/z* = 323.1881 ([M + H]⁺, calcd for C₁₉H₂₃N₄O 323.1872) ppm.

1-[4-(4-Fluorophenyl)piperazin-1-yl]-1,2-propandione, 1-(2-phenylhydrazone) (3d, C₁₉H₂₁FN₄O)

Yield 2.59 g (76%); m.p.: 160–164 °C; *R*_f = 0.55; ¹H NMR (CDCl₃): δ = 9.19 (s, 1H, NH), 6.89–7.50 (m, 9H, Ar), 3.20, 3.19 (each bs, each 4H, piperazine), 2.43 (s, 3H, COCH₃); ¹³C NMR (CDCl₃): δ = 195.09 (C=O), 158.96 (C=N), 114.20, 115.48, 115.77, 118.13, 118.24, 122.31, 129.54, 142.48, 143.12, 148.12, 148.15 (Ar), 51.18, 48.08 (piperazine), 25.75 (COCH₃); IR (KBr): $\bar{\nu}$ = 3,420, 1,678, 1,537 cm⁻¹; HRMS (CI): *m/z* = 341.1780 ([M + H]⁺, calcd for C₁₉H₂₂FN₄O 341.1778) ppm.

1-(4-Methylpiperazin-1-yl)-1,2-propandione,

1-[2-(4-chlorophenyl)hydrazone] (4a, C₁₄H₁₈ClN₄O)

Yield 2.63 g (85%); m.p.: 110–112 °C; *R*_f = 0.67; ¹H NMR (CDCl₃): δ = 9.03 (s, 1H, NH), 7.25 (d, *J* = 8.8 Hz, 2H, C₆H₄Cl), 7.10 (d, *J* = 8.9 Hz, 2H, C₆H₄Cl), 3.06, 2.50 (each bs, each 4H, piperazine), 2.38 (s, 3H, NCH₃), 2.34 (s, 3H, COCH₃); ¹³C NMR (CDCl₃): δ = 194.92 (C=O), 143.75 (C=N), 115.28, 129.41, 141.28, 126.77 (C₆H₄Cl), 55.77, 47.69 (piperazine), 46.38 (CH₃), 25.76 (COCH₃); IR (KBr): $\bar{\nu}$ = 3,420, 1,678, 1,537 cm⁻¹; HRMS (CI): *m/z* = 295.1339 ([M + H]⁺, calcd for C₁₄H₁₉ClN₄O 295.1326), 297.1322 ([M + H]⁺, calcd for C₁₄H₁₉ClN₄O 297.1296) ppm.

1-(4-Ethylpiperazin-1-yl)-1,2-propandione,

1-[2-(4-chlorophenyl)hydrazone] (4b, C₁₅H₂₁ClN₄O)

Yield 2.22 g (72%); m.p.: 100–102 °C; *R*_f = 0.72; ¹H NMR (CDCl₃): δ = 9.05 (s, 1H, NH), 7.23 (d, *J* = 8.9 Hz, 2H, C₆H₄Cl), 7.09 (d, *J* = 8.9 Hz, 2H, C₆H₄Cl), 3.06, 2.51 (each bs, each 4H, piperazine), 2.44 (q, *J* = 7.2 Hz, 2H, CH₂CH₃), 2.37 (s, 3H, COCH₃), 1.09 (t, *J* = 7.2 Hz, 3H, CH₂CH₃); ¹³C NMR (CDCl₃): δ = 194.88 (C=O), 143.84 (C=N), 115.26, 129.39, 141.32, 126.69 (C₆H₄Cl), 53.57, 47.83 (piperazine), 52.59 (CH₂CH₃), 25.76 (COCH₃), 12.03 (NCH₂CH₃); IR (KBr): $\bar{\nu}$ = 3,420, 1,678, 1,537 cm⁻¹; HRMS (CI): *m/z* = 309.1475 ([M + H]⁺, calcd for C₁₅H₂₂ClN₄O 309.1482), 311.1469 ([M + H]⁺, calcd for C₁₅H₂₂ClN₄O 311.1453) ppm.

1-(4-Phenylpiperazin-1-yl)-1,2-propandione,

1-[2-(4-chlorophenyl)hydrazone] (4c, C₁₉H₂₁ClN₄O)

Yield 3.03 g (85%); m.p.: 145–150 °C; *R*_f = 0.60; ¹H NMR (CDCl₃): δ = 9.16 (s, 1H, NH), 6.92–7.32 (m, 5H, C₆H₅), 7.27 (d, *J* = 8.8 Hz, 2H, C₆H₄Cl), 7.13 (d, *J* = 8.8 Hz, 2H, C₆H₄Cl), 3.27, 3.25 (each bs, each 4H, piperazine), 2.43 (s, 3H, COCH₃); ¹³C NMR (CDCl₃): δ = 150.96 (C=O), 143.46 (C=N), 114.82, 115.40, 116.71, 116.94, 117.35, 120.65, 126.94, 127.62, 129.08, 129.31,

129.47, 141.23, 141.39 (Ar), 50.42, 47.90 (piperazine), 25.85 (COCH₃); IR (KBr): $\bar{\nu}$ = 3,420, 1,678, 1,537 cm⁻¹; HRMS (CI): m/z = 357.1480 ([M + H]⁺, calcd for C₁₉H₂₂³⁵ClN₄O 357.1482), 359.1490 ([M + H]⁺, calcd for C₁₉H₂₂³⁷ClN₄O 359.1453) ppm.

1-[4-(4-Fluorophenyl)piperazin-1-yl]-1,2-propandione, 1-[2-(4-chlorophenyl)hydrazone] (4d, C₁₉H₂₀ClFN₄O)
Yield 3.08 g (82%); m.p.: 150–154 °C; R_f = 0.59; ¹H NMR (CDCl₃): δ = 9.13 (s, 1H, NH), 6.87–6.99 (m, 4H, C₆H₄F), 7.26 (d, J = 8.8 Hz, 2H, C₆H₄Cl), 7.11 (d, J = 8.8 Hz, 2H, C₆H₄Cl), 3.18 (bs, 8H, piperazine), 2.41 (s, 3H, COCH₃); ¹³C NMR (CDCl₃): δ = 195.00 (C=O), 159.01 (C=N), 114.36, 115.50, 115.79, 118.18, 118.28, 126.94, 129.46, 141.19, 143.49, 148.02, 155.83 (Ar), 51.15, 48.04 (piperazine), 25.81 (COCH₃); IR (KBr): $\bar{\nu}$ = 3,420, 1,678, 1,537 cm⁻¹; HRMS (CI): m/z = 375.1405 ([M + H]⁺, calcd for C₁₉H₂₁³⁵ClFN₄O 375.1388), 377.1415 ([M + H]⁺, calcd for C₁₉H₂₁³⁷ClFN₄O 377.1358) ppm.

1-(4-Methylpiperazin-1-yl)-1,2-propandione, 1-[2-(4-bromophenyl)hydrazone] (5a, C₁₄H₁₉BrN₄O)
Yield 2.68 g (79%); m.p.: 106–108 °C; R_f = 0.66; ¹H NMR (CDCl₃): δ = 6.03 (s, 1H, NH), 7.37 (d, J = 8.8 Hz, 2H, C₆H₄Br), 7.04 (d, J = 8.8 Hz, 2H, C₆H₄Br), 3.04, 2.47 (each bs, each 4H, piperazine), 2.36 (s, 3H, NCH₃), 2.31 (s, 3H, COCH₃); ¹³C NMR (CDCl₃): δ = 194.91 (C=O), 143.86 (C=N), 115.70, 132.29, 141.74, 114.09 (C₆H₄Br), 55.84, 47.79 (piperazine), 46.46 (NCH₃), 25.78 (COCH₃); IR (KBr): $\bar{\nu}$ = 3,420, 1,678, 1,537 cm⁻¹; HRMS (CI): m/z = 339.0805 ([M + H]⁺, calcd for C₁₄H₂₀⁷⁹BrN₄O 339.0820), 341.0790 ([M + H]⁺, calcd for C₁₄H₂₀⁸¹BrN₄O 341.0800) ppm.

1-(4-Ethylpiperazin-1-yl)-1,2-propandione, 1-[2-(4-bromophenyl)hydrazone] (5b, C₁₅H₂₁BrN₄O)
Yield 2.65 g (75%); m.p.: 115–120 °C; R_f = 0.71; ¹H NMR (CDCl₃): δ = 9.04 (s, 1H, NH), 7.38 (d, J = 8.8 Hz, 2H, C₆H₄Br), 7.04 (d, J = 8.8 Hz, 2H, C₆H₄Br), 3.51, 3.06 (each bs, each 4H, piperazine), 2.44 (q, J = 7.3 Hz, 2H, CH₂CH₃), 2.37 (s, 3H, COCH₃), 1.09 (t, J = 7.2 Hz, 3H, CH₂CH₃); ¹³C NMR (CDCl₃): δ = 194.91 (C=O), 143.93 (C=N), 115.69, 132.29, 141.78, 114.06 (C₆H₄Br), 53.58, 47.86 (piperazine), 52.60 (CH₂CH₃), 25.78 (COCH₃), 12.04 (NCH₂CH₃); IR (KBr): $\bar{\nu}$ = 3,420, 1,678, 1,537 cm⁻¹; HRMS (CI): m/z = 353.0954 ([M + H]⁺, calcd for C₁₅H₂₂⁷⁹BrN₄O 353.0977), 355.0945 ([M + H]⁺, calcd for C₁₅H₂₂⁸¹BrN₄O 355.0957) ppm.

1-(4-Phenylpiperazin-1-yl)-1,2-propandione, 1-[2-(4-bromophenyl)hydrazone] (5c, C₁₉H₂₁BrN₄O)
Yield 3.00 g (75%); m.p.: 148–150 °C; R_f = 0.44; ¹H NMR (CDCl₃): δ = 9.12 (s, 1H, NH), 6.93–7.32 (m, 5H, C₆H₅), 7.40 (d, J = 8.7 Hz, 2H, C₆H₄Br), 7.07 (d, J = 8.7 Hz, 2H, C₆H₄Br), 3.28 (bs, 8H, piperazine), 2.42 (s, 3H, COCH₃); ¹³C NMR (CDCl₃): δ = 195.12 (C=O),

143.50 (C=N), 114.36, 115.24, 115.79, 116.82, 116.96, 129.33, 136.16, 132.36, 141.65 (Ar), 50.51, 47.77 (piperazine), 25.84 (COCH₃); IR (KBr): $\bar{\nu}$ = 3,420, 1,678, 1,537 cm⁻¹; HRMS (CI): m/z = 401.0997 ([M + H]⁺, calcd for C₁₉H₂₂⁷⁹BrN₄O 401.0977), 403.0986 ([M + H]⁺, calcd for C₁₉H₂₂⁸¹BrN₄O 403.0957) ppm.

1-[4-(4-Fluorophenyl)piperazin-1-yl]-1,2-propandione, 1-[2-(4-bromophenyl)hydrazone] (5d, C₁₉H₂₀BrFN₄O)
Yield 3.15 g (75%); m.p.: 152–154 °C; R_f = 0.38; ¹H NMR (CDCl₃): δ = 9.12 (s, 1H, NH), 6.87–6.99 (m, 4H, C₆H₄F), 7.40 (d, J = 8.5 Hz, 2H, C₆H₄Br), 7.06 (d, J = 8.5 Hz, 2H, C₆H₄Br), 3.18 (bs, 8H, piperazine), 2.41 (s, 3H, COCH₃); ¹³C NMR (CDCl₃): δ = 195.00 (C=O), 159.02 (C=N), 114.32, 115.50, 115.76, 115.79, 118.16, 118.26, 132.36, 141.63, 143.56, 148.04, 148.07, 155.82 (Ar), 51.16, 48.06 (piperazine), 25.83 (COCH₃); IR (KBr): $\bar{\nu}$ = 3,420, 1,678, 1,537 cm⁻¹; HRMS (CI): m/z = 419.0898 ([M + H]⁺, calcd for C₁₉H₂₀⁷⁹BrFN₄O 419.0883), 421.089 ([M + H]⁺, calcd for C₁₉H₂₀⁸¹BrFN₄O 421.0862) ppm.

Cyclic voltammetry

For cyclic voltammetry, we used a Faraday MP scanning potentiostat, model F02A (Obbligato Objectives, Inc.), and experiments were carried out with the aid of a companion computer program installed on a personal computer. We constructed a planar, circular working electrode with a geometric area of 0.071 cm² by press-fitting a short length of 3-mm-diameter glassy carbon rod (Grade GC-20, Tokai Electrode Manufacturing Co., Tokyo, Japan) into a Teflon shroud. Before each cyclic voltammogram was recorded, the working electrode was cleaned on a Master-Tex (Buehler) polishing pad with an aqueous suspension of 0.05 μ m alumina, after which the electrode was rinsed ultrasonically in DMF and wiped dry before being inserted into the electrochemical cell. A reference electrode consisting of a cadmium-saturated mercury amalgam in contact with DMF saturated with both cadmium chloride and sodium chloride was employed. This reference electrode has a potential of –0.76 V versus the aqueous saturated calomel electrode (SCE) at 25 °C [27–29]; however, all potentials reported in this publication are given with respect to the SCE. A description of the cell used for cyclic voltammetry can be found in an earlier paper [30]. This single-compartment, three-electrode cell incorporates a platinum wire auxiliary (counter) electrode, along with the aforementioned working and reference electrodes.

Acknowledgments Financial support provided by Hashemite University is gratefully acknowledged. R. J. A.-J. thanks Deutsche Forschungsgemeinschaft (DFG) for a research fellowship for visiting faculty. High-resolution mass analyses were performed in the Indiana

University Mass Spectrometry Facility; the HRMS system was purchased with funds provided by the National Institutes of Health grant no. 1S10RR016657-01.

References

1. MacCoss M, Baillie TA (2004) *Science* 303:1810
2. Hanahan D, Weinberg RA (2000) *Cell* 100:57
3. Giamas G, Stebbing J, Vorgias CE, Knippschild U (2007) *Pharmacogenomics* 8:1005
4. Khalaj A, Adibpour N, Shahverdi AR, Daneshlab M (2004) *Eur J Med Chem* 39:699
5. Broekkamp CLE, Leysen D, Peeters BWMM, Pinder RM (1995) *J Med Chem* 38:4615
6. Naito H, Ohsuki S, Atsumi R, Minami M, Mochizuki M, Hirotsu K, Kumazawa E, Ejima A (2005) *Chem Pharm Bull* 53:153
7. Ibarra M, Hong E, Villalobos-Molina RJ (2000) *J Auton Pharmacol* 20:139
8. Jiang X-H, Song Y-L, Long Y-Q (2004) *Bioorg Med Chem Lett* 14:3675
9. Yoon J, Yoo EA, Kim J-Y, Pae AN, Rhim H, Park W-K, Kong JY, Choo H-YP (2005) *Bioorg Med Chem* 16:5405
10. Vu CB, Peng B, Kumaravel G, Smits G, Jin X, Phadke D, Engber T, Huang C, Reilly J, Tam S, Grant D, Hetu G, Chen L, Zhang J, Petter RC (2004) *J Med Chem* 47:4291
11. Tollefson GD, Lancaster SP, Montague-Clouse J (1991) *Psychopharmacol Bull* 27:163
12. Rotzinger S, Fang J, Baker GB (1998) *Drug Metab Dispos* 26:572
13. Wilson DM, Termin AP, Mao L, Ramirez-Weinhouse MM, Molteni V, Grootenhuys PDJ, Miller K, Keim S, Wise GJ (2002) *Med Chem* 45:2123
14. Oh YS, Yun M, Hwang SY, Hong S, Shin Y, Lee K, Yoon KH, Yoo YJ, Kim DS, Lee SH, Lee YH, Park HD, Lee CH, Lee SK, Kim S (1998) *Bioorg Med Chem Lett* 8:631
15. Lee K, Hwang SY, Hong S, Hong CY, Lee C-S, Shin Y, Kim S, Yun M, Yoo YJ, Kang M, Oh YS (1998) *Bioorg Med Chem* 6:869
16. Lee K, Jung W-H, Park CW, Park HD, Lee SH, Kwon OH (2002) *Bioorg Med Chem Lett* 12:1017
17. Clemens F, Drutkowski G, Wiese M, Froberg P (2002) *Biochim Biophys Acta* 1549:88
18. Goyal RNJ (1992) *Sci Ind Res* 51:948
19. Becker HGO, Görmär G, Timpe H-JJ (1970) *J Prakt Chem* 312:610
20. Tabaković I, Laćan M, Damoni S (1976) *Electrochim Acta* 21:621
21. Barbey G, Delahaye D, Lamant M, Caulet C (1980) *Electrochim Acta* 25:1273
22. Limacher LL, Delay FD, Bédert N, Tissot P (1989) *Helv Chim Acta* 72:1383
23. Okimoto M, Nagata Y, Takahasi Y (2003) *Bull Chem Soc Jpn* 76:1447
24. Okimoto M, Takahasi Y, Kakuchi T (2003) *Synthesis* 13:2057
25. Mamatha GP, Sherigara BS, Mahadevan KMJ (2003) *Chem Sci* 119:267
26. Hussein AQ, El-Abdelah MM, Al-Adhami KH, Abushamleh AS (1989) *Heterocycles* 29:1163
27. Marple LW (1967) *Anal Chem* 39:844
28. Manning CW, Purdy WC (1970) *Anal Chim Acta* 51:124
29. Hall JL, Jennings PW (1976) *Anal Chem* 48:2026
30. Vieira KL, Peters DGJ (1985) *Electroanal Chem* 196:93